CFD MODELING OF GEOMAT PROTECTED ABUTMENTS

H. Hosseini[1], N. Hataf[2], and N. Talebbeydokhti[3]

[1]MSc. Student of Hydraulic Structures / Dept. of Civil & Environmental Engineering, Shiraz University, Shiraz, Iran; Tel: +98-917 714 5834; Fax: +98-711 647 3039; Email: hajar_h26@yahoo.com,

[2]Proffesor / Dept. of Civil & Environmental Engineering, Shiraz University, Shiraz, Iran; Tel: +98-711 613 3108; Fax: +98-711 647 3039; Email: nhataf@shirazu.ac.ir

[3]Proffesor / Dept. of Civil & Environmental Engineering, Shiraz University, Shiraz, Iran; Tel: +98-711 613 3018; Fax: +98-711 647 3039; Email: taleb@shirazu.ac.ir

ABSTRACT

Scour at bridge abutments is one of the most prevalent causes of bridge failure and result in disturbance in traffic and even loss of life. In order to control the bridge abutment scour, there are two countermeasures: first, mechanical stabilization by using protection units like riprap, gabions, cable tied blocks and etc., and the second is flow altering units like guide banks, dikes, spurs and so on. Recently use of geobags and geomats instead of traditional materials spread widely in controlling scour around hydraulic structures. Geobags are geotextile cloth bags filled with dredged materials, sand or concrete. Because of low cost, easy performance and availability, geobags and geomats are good supersedences for other countermeasures like riprap. This paper presents a Computational Fluid Dynamics (CFD) modeling of bridge abutment scour protection by using geomats. The model has been used to solve three dimensional, transient, Navier-Stokes equation. A nonlinear RNG turbulence model was used for modeling of the flow field near the abutment, where horseshoe vortices are formed and the turbulent flow is more dominant. The influence of geomats' geometry in controlling vertical wall abutments scour has been studied. The results showed that, geomats may protect the abutment itself from scouring well, but the scour may shift to the downstream of the abutment.

Keywords: Bridge abutment, scour, geomat, CFD

INTRODUCTION

One of the most important causes of bridge failure is abutment scour. Scour is a natural phenomenon that happens due to sediment transport near the structure or turbulent flow. According to Kwan (1988) and Kwan and Melville (1994), a primary vortex due to the down-flow motion upstream side of the abutment, which is similar to the horseshoe vortex at piers, is the main cause of abutments scour. They also, identified a secondary vortex in counter-rotational direction with the primary vortex, which is believed to have a reduction effect on the primary vortex erosion capacity. There are many methods and countermeasures for controlling abutment scour. These methods can be divided in two categories: mechanical stabilization by using protection units and flow altering units. In mechanical stabilization, an additional armor layer acts against hydraulic shear stress and prevents erosion. Changing of the flow properties and thus reducing abutment scour is the objective of flow altering units. Lagasse et al. (2007) and Barkdoll et al. (2007) had a comprehensive study about all the methods and countermeasures of controlling bridge scour. The most common bed armoring layer is riprap (Luachlan and Melville, 2001). Some units of flow altering are sacrificial sill (Cheiw and Lim, 2003), collars and slots (Kumar et al., 1999 and Zarrati et al., 2006) and parallel walls (Li et al., 2006). In recent decades, geobags are used in controlling hydraulic and marine structures scour (Heibaum, 2002 and pilarczyc, 2000). Geobags are geotextile cloth bags that filled with dredged materials, sand or concrete. They are used instead of riprap or another layers of bed armoring, but rarely used for controlling bridge abutment scour. Because of low price, easy performance and availability, geobags are good supersedence for other countermeasures like riprap.

The studies of abutment scour had been started by laboratory researches. There are many parameters affecting the abutment scour. Accordingly, by use of dimensional analysis, multiple relations for abutment scour depth had been derived (Garde et al., 1961; Melville, 1992; Sturm and Janjua, 1994; Lim 1997). In addition to laboratory researches, numerical modeling is also used in studding turbulent flow and sediment transport around bridge abutments. Bakker (1974) derived a numerical model for prediction of suspended sediment concentration. Hagatun et al., (1986) presented a turbulent model for simulation of simultaneous sediment concentration and turbulent boundary layer in sheet flow regime over a flat bed. Olsen et al.,

(1993) predicted the developing process of local scour by using three dimensional flow and sediment transport. Richardson and Pancheng (1998) simulated the flow structure near bridge piers with and without scour hole. In comparison to laboratory simulation data, they found that FLOW 3D hydrodynamic model predicts flow properties near bridge piers. Tseng et al. (2000) preformed a numerical modeling of square and circular piers by using large-eddy simulation (LES). They found that the down flow is made at the front face of the pier and this affects the creation of the horseshoe vortex. Esmaeili et al., (2009) used a CFD model, SSIIM program to investigate local flow and sediment transport around bridge piers. Their results showed that the program can simulate the flow patterns and scouring around the piers well. They also found the κ-ω turbulent model gives more reasonable results. Koken and Gogus (2010) simulated the turbulent flow and horseshoe vortices around the abutment and investigated the abutment length effect on the bed shear stress. By use of laboratory and numerical modeling, Morales and Ettema (2011) presented a relationship for predicting the optimum mesh size for depth-averaged models of flow around abutments and similar hydraulic structures.

In this paper, the influence of geomats (large geobags) on controlling bridge abutments scour is studied by FLOW 3D. The model has been used to solve three dimensional, transient, Navier-Stokes equation. A turbulent RNG model is used to model the flow field and vortex shedding in vicinity of the abutment. The primary simulation results had been compared with laboratory data of Kayaturk (2005) and have shown a good agreement.

GOVERNING EQUATIONS

Hydrodynamic Model

The commercial CFD code, FLOW 3D is based on finite difference. This model is capable of fluid-boundary and the fluid-fluid and fluid-air interfaces simulation with rectangular non boundary fitted coordinate. Its hydrodynamic model solves three-dimensional Reynolds Navier-Stokes equation and the continuity equation simultaneously. The continuity equation (1) and the Navier-Stokes equation for incompressible fluid (2) are as follows (FLOW 3D user's manual):

$$\frac{\partial}{\partial x_i} u_i A_i = 0 \tag{1}$$

$$\frac{\partial u_i}{\partial t} + \frac{1}{V_f}\left(u_j A_j \frac{\partial u_i}{\partial x_j}\right) = -\frac{1}{\rho}\frac{\partial P}{\partial x_i} + G_i + f_i - Ku_i \tag{2}$$

where:

$$\rho V_f f_i = \omega s_i - \left[\frac{\partial}{\partial x_j}(A_j S_{ij})\right] \tag{3}$$

$$S_{ii} = -2\mu_{tot}\left[\frac{\partial u_i}{\partial x_i}\right]$$

$$S_{ij} = -\mu_{tot}\left[\frac{\partial u_i}{\partial x_j} + \frac{\partial u_j}{\partial x_i}\right]$$

where u_i = mean velocity; P = pressure; A_i = fractional area open to the flow in the i direction; V_f = fractional volume open to the flow; G_i are body accelerations; f_i are viscous accelerations; K is the sediment inter-granular drag term; S_{ij}=strain rate tensor; ωs_i = wall shear stress; ρ = density of water; μ_{tot} = total dynamic viscosity, which include the effects of turbulence ($\mu_{tot}=\mu+\mu_T$); and μ_T is eddy viscosity.

For simulation of the turbulent flow around the abutment the standard turbulent *RNG* model is used. The *RNG* model approximates the eddy viscosity as follows:

$$\mu_T = \frac{\rho C_\mu k^2}{\varepsilon} \tag{4}$$

k is turbulent kinetic energy and ε is dissipation rate. The closure equation for k and ε are given by:

$$\frac{\partial k}{\partial t} + u_j \frac{\partial k}{\partial x_j} = \tau_{ij}\frac{\partial u_i}{\partial x_j} - \varepsilon + \frac{\partial}{\partial x_j}\left[\left(\nu + \frac{\nu_T}{\sigma_k}\right)\frac{\partial k}{\partial x_j}\right] \tag{5}$$

$$\frac{\partial \varepsilon}{\partial t} + u_j \frac{\partial \varepsilon}{\partial x_j} = C_{\varepsilon 1}\frac{\varepsilon}{k}\tau_{ij}\frac{\partial u_i}{\partial x_j} - C_{\varepsilon 2}\frac{\varepsilon^2}{k} + \frac{\partial}{\partial x_j}\left[\left(\nu + \frac{\nu_T}{\sigma_\varepsilon}\right)\frac{\partial \varepsilon}{\partial x_j}\right] \tag{6}$$

The *RNG* model uses equations similar to the equations for the *k-ε* model. However, equation constants that are found empirically in the standard *k-ε* model are derived explicitly in the *RNG* model. The boundary conditions for the k and ε equations are defined with logarithmic law of the wall formulation as follows:

$$k = \frac{u_*^2}{\sqrt{C_\mu}}, \varepsilon = \frac{u_*^3}{\kappa y_0} \tag{7}$$

where u_* is the shear velocity and solved iteratively by the combined smooth and rough logarithmic law of wall equation given by

$$u_0 = u_*\left[\frac{1}{\kappa}ln\left(\frac{\rho u_* y_0}{\mu + \rho a u_* k_s}\right) + 5.0\right] \tag{8}$$

In the above equations, κ= von Karman constant; a=constant (=0.247); y_0=distance from the solid wall to the location of the tangential velocity, u_0, and k_s=roughness. The wall shear stress, ωs_i, is determined by

$$\omega s_i = \sum_j \frac{2\rho|u_{*i}|u_{*i}}{\Delta x_j} \tag{9}$$

The computed wall shear stress, ωs_i, is directly used in the solution of momentum equation through Eq. (3).

For tracking the fluid-fluid and fluid-air interfaces, FLOW 3D uses the technique of volume of fluid (VOF). In this technique, a single variable F (fluid fraction) is assigned to each cell that has a value of 1.0 if the cell is filled completely by fluid and a value of 0.0 if the cell is completely empty. Thus, if a cell has a value of F between 0.0 and 1.0 then the cell contains a free surface. For simulation of the interfaces with solid boundaries, it uses fractional area-volume obstacle representation (FAVOR) method. This method calculates the open cell areas and volumes in each rectangular cell to determine the obstacle occupation regions.

Scour Model

The FLOW 3D sediment scour model can predict transportation of packed and suspended sediment. The model has two important modulus, drifting and lifting (Brethour, 2003). The drifting modulus produces the driving force on the sediment particle to be suspended in the flow, which is called the drift-flux model. Lifting modulus acts as the lift force caused by local shear stress to separate the particles from the bed. The drag term, K, in momentum equation is defined by:

$$K = \begin{cases} 0 & f_s < f_{s,co} \\ \left(\frac{f_{s,cr} - f_{s,co}}{f_{s,cr} - f_s}\right)\left(\frac{f_{s,cr} - f_{s,co}}{f_{s,cr} - f_s} - 1\right) & f_{s,co} < f_s < f_{s,cr} \\ \infty & f_s > f_{s,cr} \end{cases} \tag{10}$$

where f_s is the solid fraction in the cell, $f_{s,co}$ is the cohesive solid fraction over which the interaction among particles occurs and fluid viscosity does not increase with the sediment concentration and $f_{s,cr}$ is the critical solid fraction over which the fluid flow ceases and behaves as the solid mass

By using a Stokes formulation, the drift and settling length scale (L_{drift}) of suspended sediment is

$$L_{drift} = \frac{f_l d^2}{18\mu}\frac{\nabla P}{\overline{\rho}}(\rho_s - \rho_l) \tag{11}$$

Where d_{50} is the average particle diameter; ρ_s is the sediment density; ρ is the fluid density; Δt is the time step; and   is the local density and given by

$$\overline{\rho} = \rho_l + f_s(\rho_s - \rho_l) \tag{12}$$

The lift length calculated at the interface of the packed bed is

$$L_{lift} = \alpha n_s \sqrt{\frac{\tau - \tau_{cr}}{\overline{\rho}}} \tag{13}$$

where n_s is the unit vector normal to the bed; τ is the magnitude of shear stress at the interface; and τ_{cr} is the critical shear stress. The critical shear stress is computed from the critical Shields number, $\theta_{cr,}$

$$\theta_{crit} = \frac{\tau_{crit}}{g(\rho_s - \rho_l)d} \tag{14}$$

The mean fluid viscosity is enhanced by the suspended sediment. This enhancement and a linear drag term for inter-granular collision for packed sediment is added to momentum equation.

MODEL SETUP

Kayaturk (2005) conducted a series of experiments to explore the abutments scour. In this paper, his laboratory flume was selected for further simulation and investigation of geomat layer efficiency in reduction of abutment scour. Acordingly, a rectangular flume with transport walls 10 m long, 1.5 m width, filled with sediment having a uniform diameter 1.48 mm and vertical wall abutment length L_a= 20 cm and width B_a= 10 cm was simulated as can be seen in Fig. 1. The flow condition for the model is as follows. The upstream flow depth is 0.1 m and the discharge is 0.05 m³/s. The downstream flow depth is set to be 0.1 m to simlate the outlet control gate. The top boundary of the domain is the atomosphere with zero pressure and at the surface of obejects, wall boundary condition are used. The procedure of simulation includeds two sub-simulation. In the firs sub-simulation, the Shields parameter of sediment bed is set to large number of 100, such that the local velocity in the vicinity of the bed interface becomes log-law velocity distribution; otherwise, the none-fully developed flow lead to disterbance in threshold motion of sediment particles. Then, by use of technique of 'restar', the first sub-simulation is utilized as the initial condition of the second sub-simulation by the real sediment Shilds parameter of 0.038. The fisrt sub-simulation duration is 150 second and flow domain reaches the steady status and the second sub-simulation duration is 60 second. A uniform rectangular mesh size of 1 cm in three directions was selected except in bed interface vertical cells size. If the vertical cell size on the interface of the sediment bed is too large, the velocity gradient closed to the bed will not be reasonable and may result in the incorrect shear stress distribution and maximum scour depth. Hence, in 2 cm of the bed interface, four mesh types was selected as fine, medium, large and very large

with vertical cell size of 0.33, 0.57, 0.67 and 1.17 cm respectively.
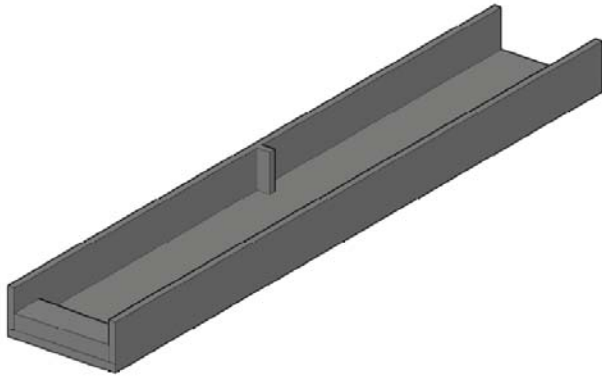

Fig. 1 Simulation flume model

SIMULATION RESULTS AND DISCUSSIONS

Simulations were firstly carried out without any protection layer and the maximum scour depth had been compared with the maximum scour depth of laboratory result, 14 mm, after 60 second (table 1). As can be seen in table 1, the large mesh type in bed interface predicts the maximum scour depth with a smaller error, so this interface mesh type was selected for other simulations.

Table 1 The maximum scour depth for four different interface mesh types

Interface mesh type	Maximum scour depth of simulation model (cm)	RE %
Fine	18.3	23
Medium	16.7	16
Large	15	7
Very large	20	30

The schematic figure of formation of abutment scour hole is shown in Fig. 2. The scour hole formed at the upstream side of the abutment as expected.
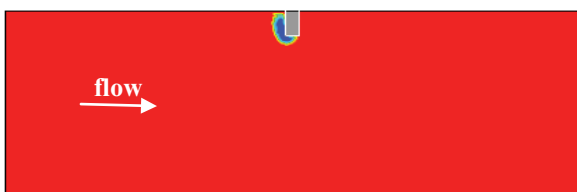

Fig. 2 Formation of scour hole at the upstream side of the abutment (plan view)

After that, abutments protected by geomats were simulated. A large geobag (geomat) has a flat profile and rounded edges, thereby reducing local acceleration of flow velocities around the geomat. Also, a geomat essentially provides its own filter cloth base as well as acts as an armoring layer. A further possible advantage of a geomat is the prospect of making a geomat that conforms to a desired shape and size for particular abutment sites (NCHRP report 578, 2007). For investigation of the efficiency of geomat layer in reduction of scour around the abutments, two geometry cases were selected. In case 1, the geomat layer is located only at front side of the abutment and in case 2, the geomat layer is located at all sides of the abutment (Fig. 3). According to Pilarszyc's relation (2002), the geomat thickness was selected to be 20 mm. its length is 300 mm and its width is 200 mm.
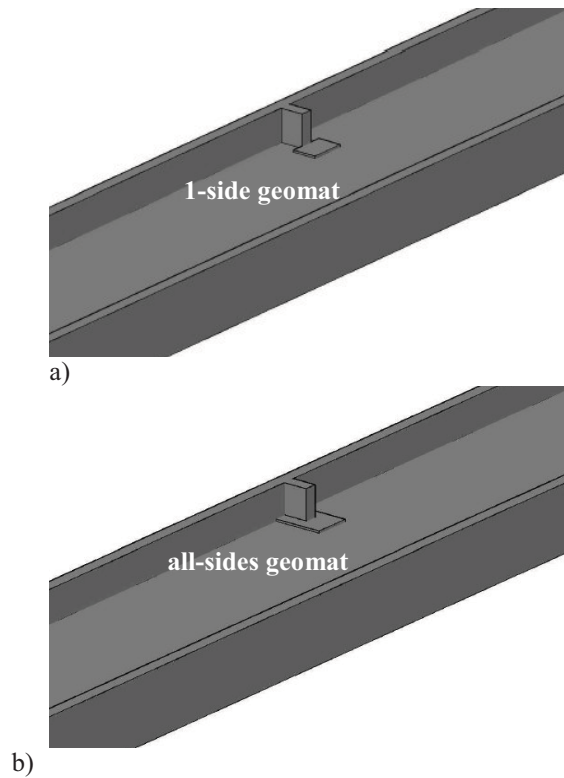

a)

b)

Fig. 3 The protected abutment with a) front side geomat layer; b) all sides geomat layer

In primary simulations, it was seen that if the total thickness of the geomat layer has been located on the sediment bed, the scour hole would developed beneath the geomat layer and reaches the abutment sides. So, half of the geomat layer thickness has been located beneath the sediment bed to prevent formation of the scour hole around the abutment. Fig. 4 shows a comparison between the 1-side protected abutment and 3-side protected one.
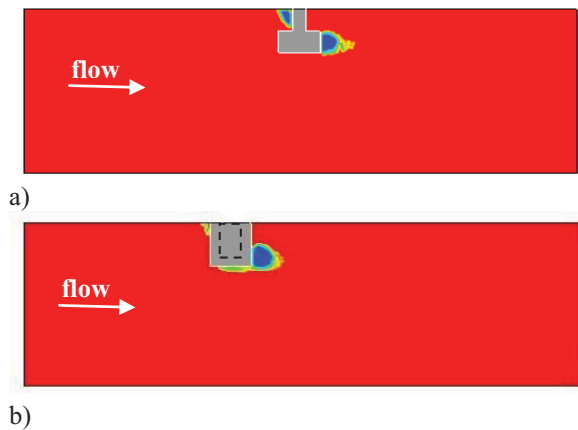
a)

b)

Fig. 4 Scour holes formation a) at the upstream side of the abutment and downstream side of the geomat layer; b) at the upstream and downstream sides of the geomat layer (plan view)

In case 1, scour holes form at the upstream side of the abutment and downstream side of the geomat layer. While in case 2, the abutment itself is protected completely, but the scour holes form at the upstream and downstream sides of the geomat leyer. The maximum scour depth comparison between 2 cases and the unprotected abutment (Table 2), shows that 3-sides geomat layer protects the abutment completely, but the scour hole shifted to downstream of the layer. Although the 1-side geomat layer does not protect the abutment thoroughly, but the maximum scour depth reduces by 45% at the upstream side of the abutment.

Table 2 Maximum scour depth around the protected abutment

simulation	$ds_A{}^*$ (mm)	$ds_B{}^{**}$ (mm)	$ds_A/ds_{A0}{}^{***}$ (%)	ds_B/ds_{A0} (%)
abutment w/o protection	15	0	100	0
abutment with geomat in front side	8.3	8.3	55	55
abutment with geomat in all sides	5	15	33	100

*: maximum scour depth upstream side of abutment or geomat layer; **: maximum scour depth downstream side of geomat layer; ***: maximum scour depth upstream side of abutment w/o protection layer.

CONCLUSIONS

The FLOW 3D code has been used to investigate the efficiency of geomat in controlling vertical wall abutments scour. The results showed good quantitative and qualitative agreement with laboratory results. Two geometry of geomat layer has been explored: case 1, the geomat layer was located at front side of the abutment and case 2, the geomat layer was located at all sides of the abutment. Simulation results showed that the scour eliminates around the abutment protected in all sides, but the scour hole shifts to the downstream of the geomat layer. Although the front side geomat layer cannot protect the abutment thoroughly, but the maximum scour depth will reduce considerably.

REFERENCES

Bakker WT. (1974). Sand concentration in an oscillatory flow. Proc. 14th Conference Coastal Engineering ASCE, Copenhagen: 1129–48.

Barkdoll, B. D., Ettema, R., Melville, B. W. (2007). Countermeasures to Protect Bridge Abutments from Scour. National Cooperative Highway Research Program (NCHRP) Rep. No. 587, Transportation Research Board, Washington, D.C.

Brethour J. M. (2001). Transient 3-D model for lifting, transporting and depositing solid material. Proc. 2001 Intl. Symp. on Environmental Hydraulics, Tempe, Arizona.

Chiew, Y.M., Lim, S.Y. (2003). Protection of bridge piers using a sacrificial sill. Proc. Inst. Civ. Eng., Waters. Maritime Energ., 156(1): 53–62.

Esmaili T, Deghani A.A, Zahiri A.R, Suzuki K. (2009). 3D numerical simulation of scouring around bridge piers (case study: bridge 524 crosses the Tanana River). World Academy of Science, Engineering and Technology 58

Flow Science, Inc. (2008). FLOW-3D User's Manual, 9.3 Editions, Flow Science, Inc., Santa Fe, N.M., U.S.A.

Garde R. J, Subramanya K, Nambudripad K. D (1961). Study of scour around spur-dikes. Journal Hydraulic Div., ASCE, 87:23–37

Heibaum, M.H (2000). Geosynthetic containers— a new field of application with nearly no limits. Proc. 7th Intl. Conf. on Geosynthetics. 7 ICG-NICE, France, 3: 1013–1016.

Hagatun K, Eidsvik KJ. (1986). Oscillatory turbulent boundary layers with suspended sediments. Journal Geophysic Res; 91(C11):13,045–55.

Kayaturk S.Y. (2005). Scour and Scour Protection at Bridge Abutments. M.S Thesis, The Middle East Technical University.

Koken M., Gogus M. (2010). Effect of abutment length on the bed shear stress and the horseshoe vortex system. Proc. International Conference on Fluvial Hydraulics, Braunschweig, Germany.

Kumar V., Ranga Raju K. G., Vittal N. (1999). Reduction of local scour around bridge piers using slots and collars. Journal Hydraulic Eng., 125(12): 1302–1305.

Kwan T. F (1988). A Study of Abutment Scour. Rep. No. 451, School of Engineering, University of Auckland, Auckland, New Zealand.

Kwan T. F, Melville B. W (1994). Local scour and flow measurements at bridge abutments, Journal Hydraulic Res. 32: 661–67.

Lauchlan, C. S., Melville, B. W. (2001). Riprap protection at bridge piers, Journal Hydraulic Eng., 127(5): 412–418.

Lagasse, P. F., Clopper, P. E., Zevenbergen, L. W., and Girard, L. G. (2007). Countermeasures to Protect Bridge Piers from Scour. National Cooperative Highway Research Program (NCHRP) Rep. No.593, Transportation Research Board, Washington, D.C.

Li H., Barkdoll B. D., Kuhnle R., Alonso C. (2006). Parallel walls as an abutment scour countermeasure, Journal Hydraulic Eng., 132(5), 510–520.

Lim S. Y (1997). Equilibrium clear-water scour around an abutment. J. Hydraul. Eng., Am. Soc. Civ. Eng. 123: 237–243

Melville B. W (1992). Local scour at bridge abutments, Journal Hydraulic Eng., ASCE, 118: 615–631.

Morales R, Ettema R (2011). Insights from Depth Averaged Numerical Simulation of Flow at Bridge Abutments in Compound Channels, Iowa University.

Olsen NRB, Melaaen MC. (1993). Three-dimensional calculation of scour around cylinders. Journal Hydraulic Eng, 119(9):1048–54.

Pilarczyc K.W (2000). Geosynthetics and Geosystems in Hydraulic and Coastal Engineering, A.A. Balkema, Rotterdam.

Sturm T. W, Janjua N. S (1994). Clear-water scour around abutments in floodplains. Journal Hydraulic Eng., ASCE, 120: 956–972.

Richardson J.E, Pancheng V.G. (1998).Three dimensional simulation of scour inducing flow at bridge piers. Journal Hydraulic Eng ASCE,: 124(5).

Tseng M, Yen CL, Song CCS. (2000). Computation of three-dimensional flow around square and circular piers. Intl. Journal Numer Meth Fluids, 34: 207–27.

Zarrati A. R., Nazahira M., Mashahir, M. B. (2006). Reduction of local scour in the vicinity of bridge pier groups using collars and riprap. Journal Hydraulic Eng., 132(2): 154–162.